University of Baghdad
College of Engineering
JE
JOURNAL OF ENGINEERING

Journal of Engineering

journal homepage: www.joe.uobaghdad.edu.iq

Volume 29 Number 10 October 2023

Controlling the Unbalanced Voltages of a Series-Connected Lead-Acid Batteries in a PV Power Storage System using Dynamic Capacitor Technique

Fadhil T. Aula

Control and Renewable Power Systems, College of Engineering, Salahaddin University, Erbil, Iraq
fadhil.aula@su.edu.krd

ABSTRACT

Lead-acid batteries have been used increasingly in recent years in solar power systems, especially in homes and small businesses, due to their cheapness and advanced development in manufacturing them. However, these batteries have low voltages and low capacities, to increase voltage and capacities, they need to be connected in series and parallel. Whether they are connected in series or parallel, their voltages and capacities must be equal otherwise the quality of service will be degraded. The fact that these different voltages are inherent in their manufacturing, but these unbalanced voltages can be controlled. Using a switched capacitor is a method that was used in many methods for balancing voltages, but their responses are slow. To increase the response and control of the balancing process, this research proposes a novel technique that consists of a dynamic capacitor for controlling the unbalanced voltages of series-connected lead-acid batteries. The proposed technique uses a main capacitor and an inductor with two switches their on/off states are controlled through a pulse width modulation. The technique is designed and validated using MATLAB/Simulink and the results for different cases are compared with other techniques such as switched capacitor technique. Results show that the proposed method promised the balancing control in a shorter time and better performance than other techniques which are crucial in the battery's voltage balancing.

Keywords: PV power system, Lead-acid battery, Voltage balancing control, Dynamic capacitor.

*Corresponding author
Peer review under the responsibility of University of Baghdad.
https://doi.org/10.31026/j.eng.2023.10.10

Article received: 12/02/2023
Article accepted: 20/05/2023
Article published: 01/10/2023

التحكم في الفولتية غير المتوازنة لبطاريات الرصاص الحمضية المتصلة بالسلسلة في نظام تخزين الطاقة الشمسية باستخدام تقنية المكثفات الديناميكية

فاضل توفيق عولا

أنظمة التحكم والطاقة المتجددة، كلية الهندسة، جامعة صلاح الدين، أربيل، العراق

الخلاصة

تستخدم بطاريات الرصاص الحامضية بشكل متزايد في السنوات الأخيرة في أنظمة الطاقة الشمسية ، خاصة في المنازل والشركات الصغيرة بسبب رخص ثمنها والتطور المتقدم في تصنيعها. ومع ذلك ، فإن هذه البطاريات ذات جهد منخفض وسعة منخفضة ، لزيادة الجهد والقدرات ، يجب توصيلها على التوالي والتوازي. سواء كانت متصلة على التوالي أو التوازي ، يجب أن تكون الفولتية والقدرات متساوية وإلا ستنخفض جودة الخدمة. حقيقة أن هذه الفولتية المختلفة متأصلة في تصنيعها ، ولكن يمكن التحكم في هذه الفولتية غير المتوازنة. يعد استخدام السعة المبدلة طريقة مستخدمة في العديد من الطرق لموازنة الفولتية ، لكن استجاباتها بطيئة. لزيادة الاستجابة والتحكم في عملية الموازنة ، تم اقتراح تقنية مكثف ديناميكي في هذا البحث للتحكم في الفولتية غير المتوازنة لبطاريات الرصاص الحامضية ذات ربط التوالي. تستخدم التقنية المقترحة السعة الرئيسية والتحريض مع مفتاحين يتم التحكم في حالات التشغيل / الإيقاف من خلال تعديل عرض النبضة. صممت هذه التقنية والتحقق من صحتها باستخدام MATLAB / Simulink وتم مقارنة النتائج بتقنيات أخرى مثل تقنية مكثف التبديل. تظهر النتائج أن الطريقة المقترحة ادت الى ضبط التوازن في وقت أقصر وبأداء أفضل من التقنيات الأخرى التي تعتبر حاسمة في موازنة جهد البطارية.

الكلمات المفتاحية: نظام الطاقة الشمسية ، بطارية الرصاص الحامضية ، التحكم في موازنة الجهد ، المكثف الديناميكي.

1. INTRODUCTION

Recently, the demand for photovoltaic (PV) technology in producing electricity has increased substantially **(Victoria et al., 2021; Zhang et al., 2021; IEA, 2022)**. On the other hand, the continuously reducing costs for building PV power plants make them successfully be used to supply electricity not just for large areas but for small businesses and households as well. However, the intermittency behavior of PV power systems especially during the night and cloudy days remains the main drawback of them. A battery storage system is counted as one of the best practical solutions to the PV drawback **(Salameh et al., 2022; Apribowo, 2022)**. In the last decade, the growth of PV power systems and the development of electric vehicles have made huge progress in adopting new technologies for manufacturing different types of batteries **(Chen et al., 2020)**. Batteries now have more charge/discharge cycles, longer life, stronger, higher capacities, and low costs **(Lipu et al., 2022; Pan et al., 2022)**. However, these batteries are still available in low voltage mostly 12 DC voltage that need to use more batteries in series and parallel connection combination to increase their voltages and capacities to follow the ratings of inverters in PV power systems **(Manimekalai et al., 2013; Fortenbacher et al., 2017; Bagalini et al., 2019, Wu et al., 2022)**.
One of the most drawbacks of almost all types of batteries is self-discharging. This self-discharging reduces battery voltage and its impact will be worse when batteries are connected in series and parallel. This impacts the operation of inverters, decreases the

storage capacity, decreases cycle charging/discharging, and shortens the battery's life. In general, parallel operation of batteries may balance their voltages to the level that all have the same voltage. While in series connecting, self-balancing does not achieve, therefore, an external procedure is required to maintain the same voltage of all batteries **(Wang, et al. 2017)**.

Different techniques have been used for equalizing batteries' voltages. **(Kim, et al., 2014)** presented a switched capacitor and the method was applied to lithium-ion batteries. **(Ye, et al., 2017)** proposed a series of switched-capacitors for battery and super-capacitor balancing strings and to increase the speed of balancing different topologies were proposed with resistors. A bi-directional Cuk converter was presented by **(Zheng et al., 2018; Rasheed, 2020)**, and a fuzzy control method was used for controlling the Cuk converter for voltage balancing of lithium-ion batteries. **(Moghaddam and Van den Bossche, 2019; Ho, et al., 2021; Wang et al., 2023)** presented different types of switched capacitor models in which these models were simulated on lithium-ion batteries operating at voltages 3 to 4.2V **(Zau et al., 2022)**. However, many studies have been done on unbalancing lithium-ion batteries but a few are dealing with lead-acid batteries. Charge equalization systems were proposed for serial lead-acid batteries in hybrid power systems **(Belmokhtar et al., 2016; Akash and Sumana, 2021)**, two systems were included: active and passive systems, the passive was based on a resistor element to remove the excess charge until matching high voltage batteries to lower voltages.

Recently, lead-acid batteries have been widely used in households' electricity storage systems due to their lower prices, and availability in different capacities, moreover, new technology in manufacturing these types of batteries makes them last longer **(Dufo-López, et al., 2021; Rajanna and Kumar, 2021)**. With the growth of using lead-acid batteries, especially in PV storage systems, and they are subjected to voltage differences during operations, therefore, an efficient voltage balancing technique is highly recommended for retaining the voltage balance of all batteries in a shorter time in low power consumption **(Geoffrey et al., 2018; Kavaliauskas et al., 2023)**.

This study proposes a dynamic capacitor technique for controlling the unbalanced voltages of lead-acid batteries which are connected in series. The proposed technique is applied on a 12V, 200Ah lead-acid battery and simulated on MATLAB/Simulink® for validating the results, and results are compared to the switched-capacitor technique. The result outcomes for different cases show that the proposed technique achieves the voltage balance in a shorter time than the other technique. The technique can be implemented on most batteries in PV power storage systems in residences and small businesses.

2. PROPOSED BALANCED BATTERY VOLTAGE SYSTEM

The proposed voltage balancing system for lead-acid batteries connected in series is depicted in **Fig. 1**. The system consists of lead-acid batteries connected in series, these batteries have the same capacities, rated voltages, same type, and same manufacturer. A voltage detector is used to detect the voltages of all batteries for any inequality. The pulse Width Modulation (PWM) controller sends signals to the switches in the dynamic capacitor according to the rate of the imbalanced voltage detection **(Alvarez et al., 2020)**. The dynamic capacitor circuit consists of the capacitor, inductor, and switches to process the balancing in the batteries' voltages.

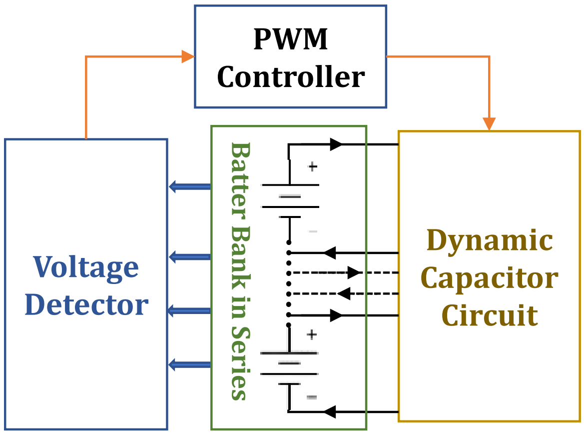

Figure 1. Block diagram of the balanced voltage system

3. LEAD-ACID BATTERY MATHEMATICAL MODEL

The equivalent mathematical model of a lead-acid battery of a cell is shown in **Fig. 2 (Raji and Kubba, 2020; Wang and Zhu,2020)**. The model is based on a 12 V 200Ah lead-acid battery. The main element of this battery is a voltage source, E_m, which represents the open circuit voltage of the state of charge for the battery. However, due to a chemical reaction inside the lead-acid battery, this open circuit voltage is overlaid by the overvoltage.
The battery open circuit voltage is given by **(Maraud et al., 2016; Hamed et al., 2018)**;

$$E_m = E_{mo} - K_e(273 + Th_e)(1 - SOC) \quad (1)$$

where K_e is the voltage temperature coefficient of the battery, Th_e is the electrolyte temperature in which ($273+Th_e$) is temperature measured in *Kelvin*, and *SOC* is the state-of-charge which is given by:

$$SOC = 1 - \frac{Q_e}{C_{10}} \quad (2)$$

where Q_e is the battery consumed charge in *Ah*, and C_{10} is the rated charge capacity of the battery in *Ah* .

The cell main branch resistors R_{i1} and R_{i2} are given by:

$$R_{i1} = -R_{10}\ln(DOC) \quad (3)$$

$$R_{i2} = R_{20}\frac{e^{A21\,(1-SOC)}}{1+e^{A22\frac{Im}{Io}}} \quad (4)$$

where R_{10}, R_{20}, A_{21}, and A_{22} are battery internal parameters and they are constant for a particular battery, I_m is the actual main branch current, I_o is the rated battery cell current, and *DOC* is the depth of charge and is given by **(Collath et al., 2022)**;

$$DOC = 1 - \frac{Q_e}{C_1} \quad (5)$$

where C_1 is the actual battery capacity under the actual discharge current and is given by:

$$C_1 = \frac{\tau_c}{R_{i1}} \quad (6)$$

where τ_c is the time constant of the cell.

The output resistance of the equivalent circuit, R_o, is given by **(Maraud et al., 2016)**:

$$R_o = R_{00}[1 + A_0(1 - SOC)] \quad (7)$$

where R_{oo} and A_o are constant parameters .

The parasitic branch current, I_p, is given by **(Maraud et al., 2016)**;

$$I_P = E_P G_{PO} e^{\frac{E_P}{E_{PO}} + A_P \frac{1-Th_e}{Th_f}} \quad (8)$$

where E_{po}, G_{po}, and A_p are battery cell constants, E_p is parasitic branch voltage, and Th_f is the electrolyte freezing temperature (-40^oC).

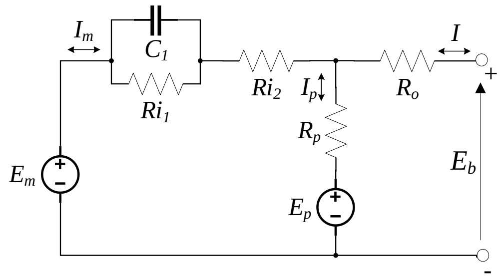

Figure 2. A cell lead-acid battery equivalent electrical circuit **(Raji and Kubba, 2020).**

4. DYNAMIC CAPACITOR

The main components of the dynamic capacitor are an inductor, L, a capacitor, C, $L_{in}C_{in}$ filter, and two switches, S_1 and S_2. The electrical circuit diagram for the dynamic capacitor is shown in **Fig. 3 (Aula, 2022).**

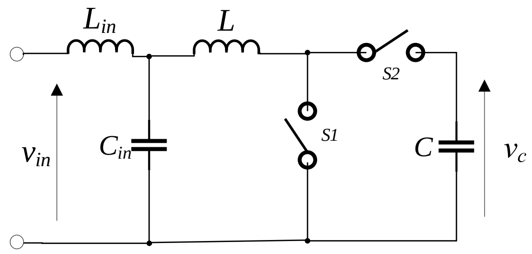

Figure 3. Dynamic capacitor circuit diagram **(Aula, 2022)**.

The capacitor voltage, v_c, can be computed from the following relationship **(Aula, 2022);**

$$v_C = \frac{1}{1-D} v_{in} \quad (9)$$

where v_{in} is the input voltage (supply voltage), and D is the duty cycle and is given by;

$$D = \frac{t_{on}}{t_{on}+t_{off}} \quad (10)$$

where t_{on} and t_{off} are switching times for both switches accounted when S_1 is *on*, S_2 is *off*, and vice versa.
The values of C and L are computed by **(Aula, 2022)**;

$$C = \frac{Q_C}{2\pi f v_C^2} \quad (11)$$

$$L = \frac{v_{in}\, x_c}{2R_f v_C} Dt \quad (12)$$

where $Q_C = \frac{v_c^2}{X_C}$, R_f is a ripple factor of the inductor current, x_c is the capacitive reactance of C, and f is the switching frequency, which is supplied by pulse width modulation (PWM).

5. CONTROLLING UNBALANCED BATTERY VOLTAGES

The principle of controlling the unbalanced voltages of batteries, in this research, is using a dynamic capacitor by dividing the LC filter according to the number of batteries in series. A proposed technique for controlling the unbalanced voltages of two series-connected batteries using a dynamic capacitor is depicted in **Fig. 4**.
The principle operation of the unbalancing voltage controller is based on four sequential modes. To simplify the analysis of these modes and since the values of L_{in} and C_{in} are very small in comparison to L and C, thus, the circuit diagram in **Fig. 4** can be simplified to one as shown in **Fig. 5**.

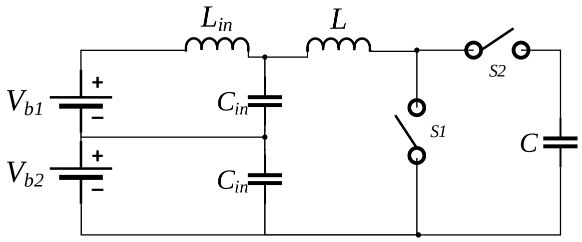

Figure 4. Series-connected two batteries controlling balancing circuit diagram.

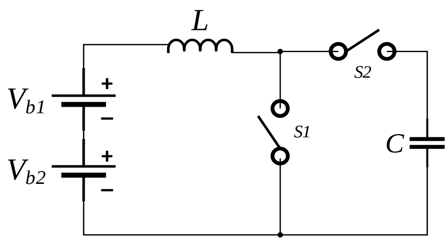

Figure 5. Simplified circuit diagram for batteries' unbalanced voltages.

Mode1

The first mode of controlling the unbalanced voltage represents switch S_1 *ON* and switch S_2 *OFF*, the simplification circuit diagram of ***mode 1*** is shown in **Fig. 6**. The current passed through the inductor, no energy storage in this mode, from both batteries can be represented as:

$$i_L(t) = \frac{1}{R_1}(1 - e^{-\frac{R_1}{L}Dt})(v_{b1} + v_{b2}) \quad (13)$$

$$v_L(t) = (v_{b1} + v_{b2})e^{-\frac{R_1}{L}Dt} \quad (14)$$

where v_{b1} and v_{b2} are battery voltages, i_L and v_L are inductor current and voltage in ***mode 1***, and R_1 is the inductor internal resistance.

Mode 2

In the second mode, switch S_1 is *OFF* and switch S_2 is *ON*, and the equivalent circuit diagram that represents this mode is shown in **Fig. 7**. The stored energy in the inductor in ***mode 1*** in time t will increase the capacitor voltage v_L, which can be expressed by the following state-space representation:

$$\begin{bmatrix} i_L \\ v_c \end{bmatrix} = \begin{bmatrix} -\frac{R_2}{L} & -\frac{1}{L} \\ \frac{1}{C} & 0 \end{bmatrix} \begin{bmatrix} i_L \\ v_c \end{bmatrix} + \begin{bmatrix} \frac{1}{L} \\ 0 \end{bmatrix} (v_{b1} + v_{b2}) \quad (15)$$

where v_c and i_L are capacitor voltage and inductor current in ***mode 2***. In which $i_L = - i_C$ (capacitor current), and R_2 is the summation of inductor and capacitor internal resistance. The eigenvalues of the system in ***mode 2*** are given by:

$$\lambda^2 + \frac{R}{L}\lambda + \frac{1}{LC} = 0 \quad (16)$$

From Eq. (16), the undamped natural frequency is 1/√LC rad/sec, and the damping ratio, ζ, is equal to $\frac{R_2}{2}\sqrt{\frac{C}{L}}$. Usually, the capacitor value is much smaller than the inductor, thus, the two eigenvalues become:

$$\lambda_{1,2} = -\frac{R_2}{2L} \pm j\sqrt{\frac{1}{LC} - (\frac{R_2}{2L})^2} \quad (17)$$

Hence, the response of the second order system and according to the damping ratio is the underdamped response which undamped natural frequency decays exponentially. The inductor current in ***mode 2*** after solving the system Eq. (15) with the assumption that capacitor voltage is initially zero can be represented by the following expression:

$$i_L(t) = i_{Lu}(t) + i_{Lf}(t) = -i_c(t) \quad (18)$$

where

$$i_{Lu}(t) = \frac{1}{R_1\sqrt{\frac{1}{LC}-(\frac{R_2}{2L})^2}} e^{-\frac{R_2}{2L}(1-D)t} [\sqrt{\frac{1}{LC} - (\frac{R_2}{2L})^2} \cos\sqrt{\frac{1}{LC} - (\frac{R_2}{2L})^2}\,(1-D)t + \frac{R_2}{L} sin\sqrt{\frac{1}{LC} - (\frac{R_2}{2L})^2}\,(1- D(t](1 - e^{-\frac{R_1}{L}t})(v_{b1} + v_{b2}) \quad (19)$$

$$i_{Lf}(t) = \frac{1}{L\sqrt{\frac{1}{LC}-(\frac{R_2}{2L})^2}}\; e^{-\frac{R_2}{2L}(1-D)t}\; sin\sqrt{\frac{1}{LC} - (\frac{R_2}{2L})^2}\;(1-D)t\,(v_{b1} + v_{b2}) \quad (20)$$

where i_{Lu} represents the unforced inductor current, i_{Lf} represents the forced current .
The capacitor voltage is given by:

$$V_c(t) = v_{cu}(t) + v_{cf}(t) \quad (21)$$

where

$$v_{cu}(t) = \frac{1}{R_1 C\sqrt{\frac{1}{LC}-(\frac{R_2}{2L})^2}} e^{-\frac{R_2}{2L}(1-D)t}\left(1-e^{-\frac{R_1}{L}t}\right) sin\sqrt{\frac{1}{LC}-(\frac{R_2}{2L})^2}\,(1-D)t(v_{b1}+v_{b2}) \quad (22)$$

$$v_{cf}(t) = \{1-e^{-\frac{R_2}{2L}(1-D)t}[cos\sqrt{\frac{1}{LC}-(\frac{R_2}{2L})^2}\,(1-D)t-\frac{R_2}{2L\sqrt{\frac{1}{LC}-(\frac{R_2}{2L})^2}}\,sin\sqrt{\frac{1}{LC}-(\frac{R_2}{2L})^2}\,(1-Dt]\}(v_{b1}+v_{b2}) \quad (23)$$

where v_{cu} represents the unforced capacitor voltage, v_{cf} is the forced capacitor voltage, and D is the duty cycle for switching *ON/OFF* as defined in Eq. (10).

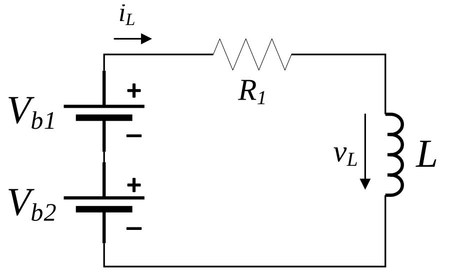

Figure 6. Mode 1 equivalent circuit diagram.

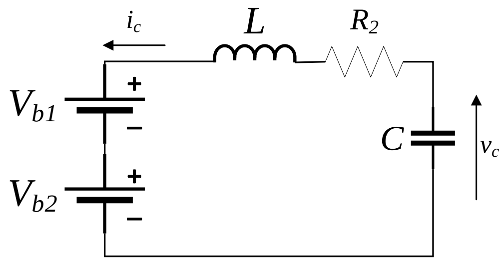

Figure 7. Mode 2 equivalent circuit diagram.

Modes 3 and 4

After the second mode in which the second cycles of switches begin, the inductor current, i_L, in Eq. (18) becomes the initial current to Eq. (13), and the same occurs for inductor voltage, v_L. Also, the capacitor voltage in Eq. (21) will be the initial capacitor voltage in the consecutive cycles. The sequence of charging/discharging capacitor voltage according to both switches, S_1 and S_2, at 5kHz PWM pulses are shown in **Fig. 8**. The switching *ON/OFF* operations which control the inductor and capacitor voltages proceed through pulse width modulation (pulses). The rate of these pulses (pulses per second) determines the inductor voltage and capacitor voltage simultaneously.

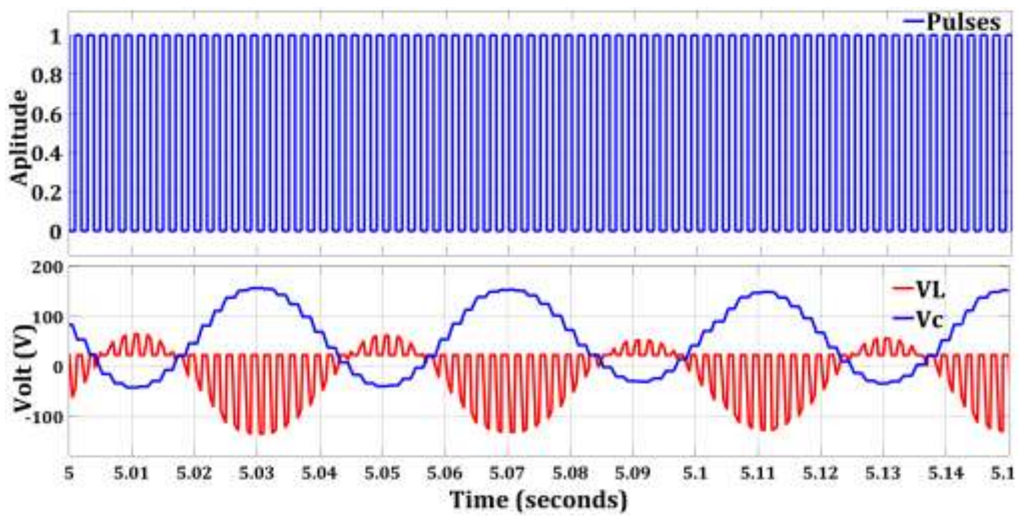

Figure 8. Capacitor and inductor voltage correspond to switch operations.

6. SIMULATION AND RESULTS

For most solar power systems, lead-acid batteries for their cost affordable, and acceptable capacities effectivity are used as backup storage. Therefore, in this research, lead-acid batteries were used with a capacity that matches the currently commercially available ones. A 12 V, 200Ah is used for all batteries throughout this research, and their parameters are given in **Table 1**. **Fig. 9** shows the MATLAB/Simulink model which is implemented for validating the model and method proposed in this research. For the optimum controlling of both switches, the PWM is chosen to be 5kHz. The inductor and capacitor values, L and C, are *3mH* and *200μF*. The internal resistances for both the inductor and capacitor are set to *0.005Ω* and *0.003 Ω*, respectively. The filter inductor and capacitor are set to *0.03mH* and *35μF*, respectively. It is wealth to note that, for filtering only one inductor is sufficient to be used, and the number of capacitors depends on the number of batteries in the series, for example, for two batteries, two filleter capacitors are used, and for four batteries in series, four filter capacitors are used, and so on. **Fig. 4** is an example of how these elements were connected to batteries .

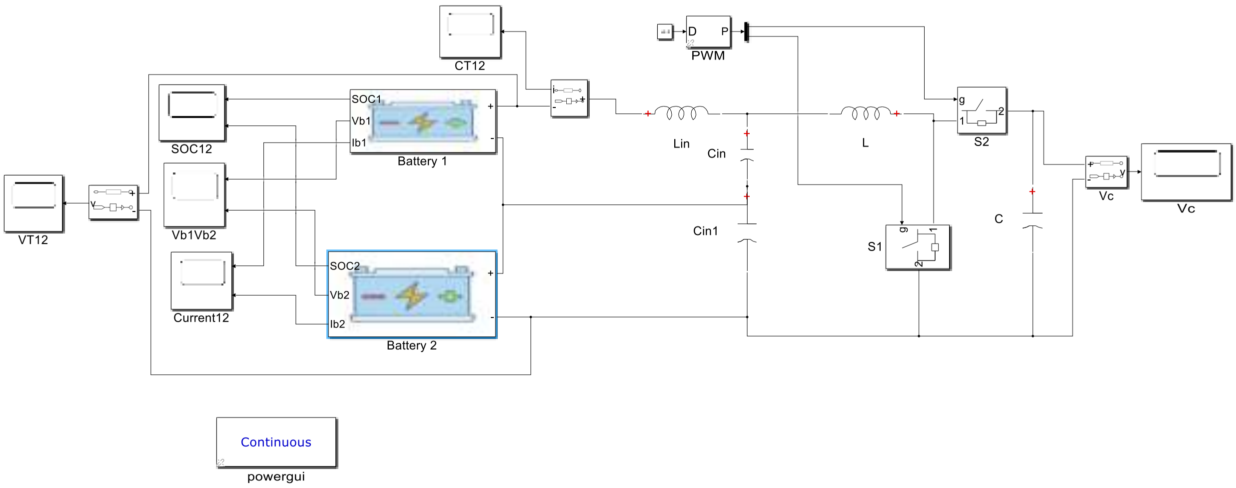

Figure 9. MATLAB simulation model for two lead-acid batteries in series with dynamic capacitor implementation.

Table 1. Assumption 12 V 200Ah lead-acid battery parameters

Parameter	Value	Parameter	Value
E_{mo}	2.18 V	R_{10}	0.2 mΩ
K_e	0.84 x 10^{-3} V/^{0}C	A_{22}	-4.225
R_{00}	1 mΩ	τ_c	7200s
G_{P0}	2 PS	R_{20}	7.5 mΩ
A_p	2	A_0	-0.2
A_{21}	-8	Th_f	-40^{o}C

For validating the proposed technique, different cases are considered. In the first case, some homes used an inverter that had a rating of 24 V battery voltage. Hence, the simulation is

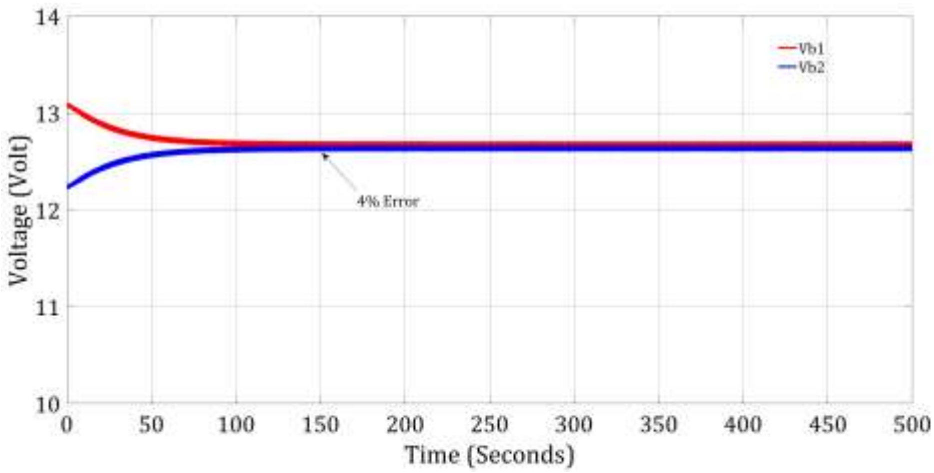

Figure 10. Balancing of two batteries' voltages connected in series for SOC 90% case.

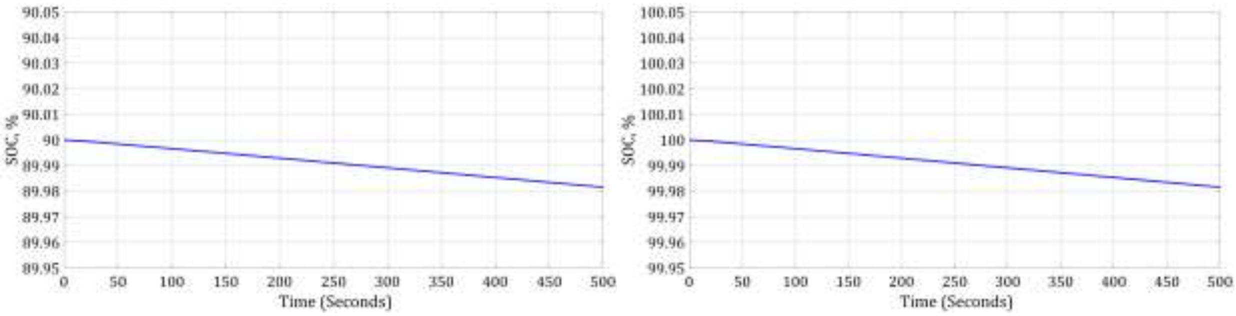

Figure 11. Batteries SOC for case 90%.

In the second case, the conditions for the first case are repeated by changing the SOC from 90% to 95%. The simulation results are shown in **Figs. 12** and **13**, respectively.

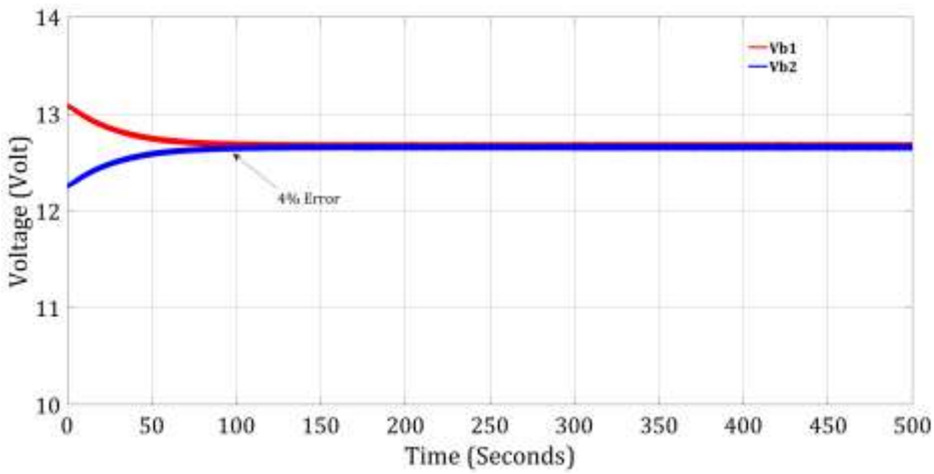

Figure 12. Balancing of two batteries' voltages connected in series for SOC case 95%.

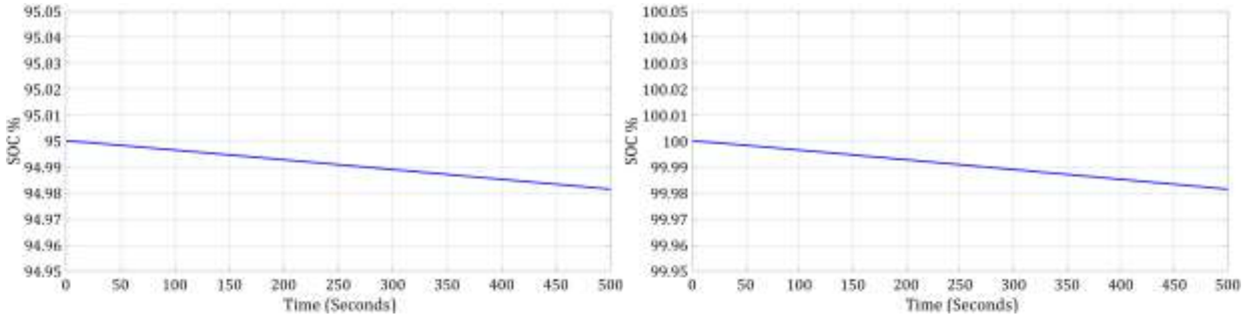

Figure 13. Batteries SOC case 95%.

In the third case, since other homes use inverters that are rated 48 V for batteries, therefore, four lead-acid batteries are used in series. Their SOCs are set as 100%, 97%, 95%, and 90%, respectively. The simulation results are shown in **Figs. 14** and **1**5.

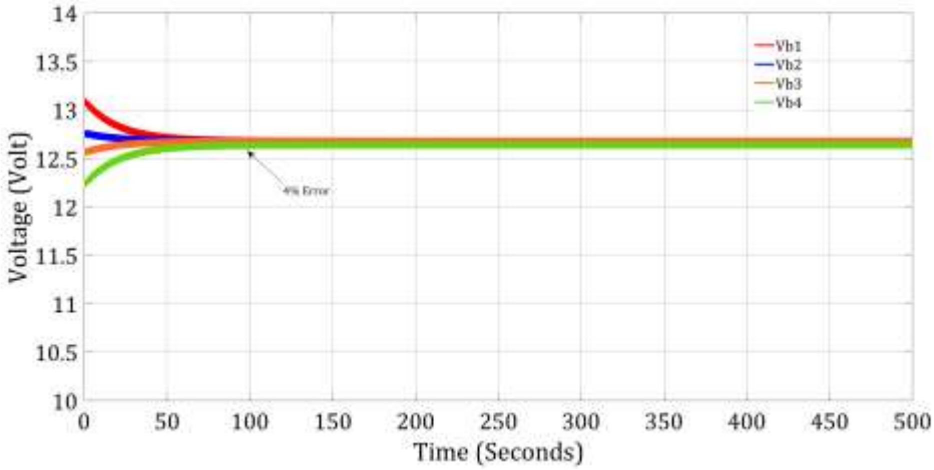

Figure 14. Balancing of four batteries' voltages connected in series.

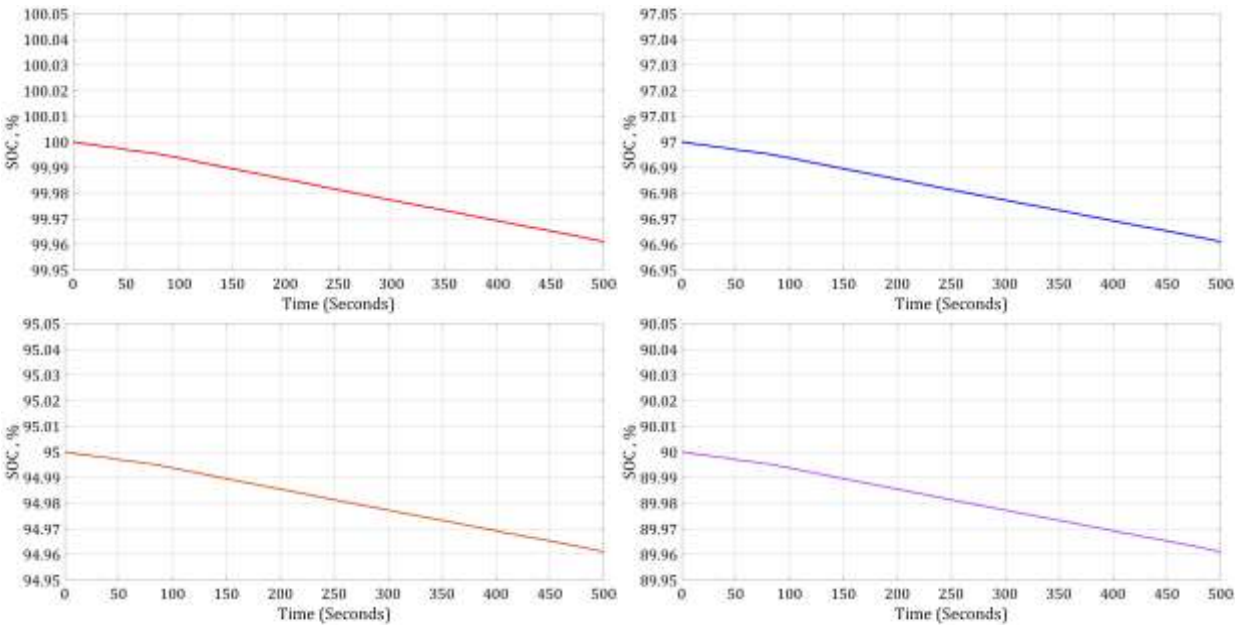

Figure 15. SOC for all four batteries during the balancing control procedure.

As depicted in all simulation results' figures, the proposed technique provided the promised results. When there are two batteries in a series, the balancing control has reached the settling time within 100 seconds for a lower than 4% error. For comparison, a switched capacitor with the same type of battery's voltage and capacity and at the same PWM frequency is tested **(Shang et al., 2017)**. The results show that the switched-capacitor technique balanced the batteries' voltages much slower and far from the result obtained in the proposed technique. **Fig.s 16, 17**, and **18** show the simulation results of the switched capacitor for balancing voltages for two and four lead-acid batteries that are connected in series. The switched capacitor method for SOC 90% and 95% after 400s was able to balance the batteries' voltages for only up to 0.6 voltage difference while it was less than 0.04 voltage and less than 100s in the proposed technique. Similarly, for four series-connected batteries, the proposed technique was faster in balancing the variation of all voltages in less time reaching less than 0.02 voltage difference in less than 100s while in the switched-capacitor after 500s of operation, the difference of voltages still more than 0.2 voltage.

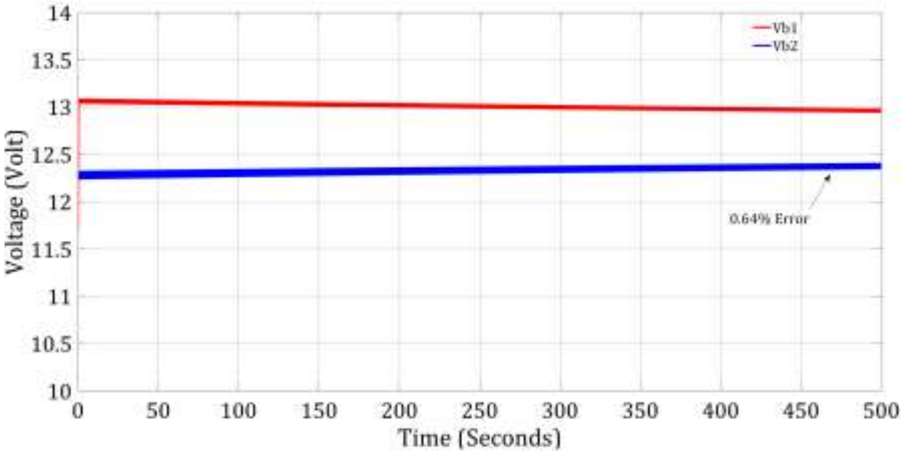

Figure 16. Two series connected batteries for SOC 90% for switched-capacitor technique.

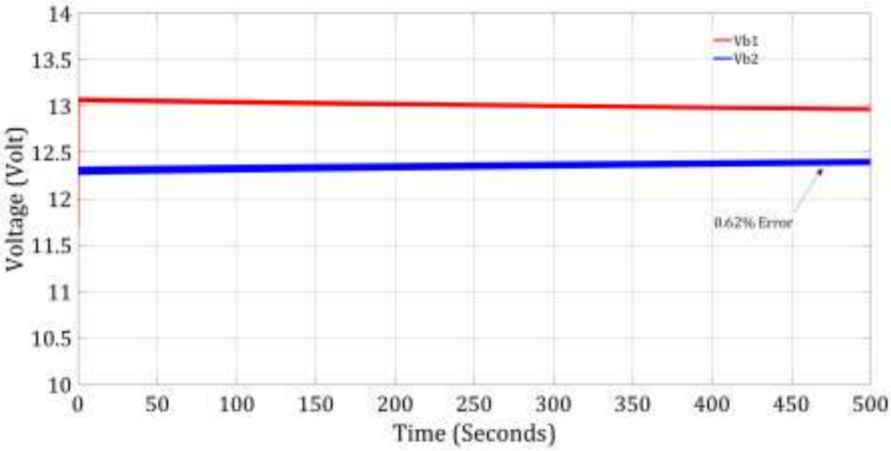

Figure 17. Two series connected batteries for SOC 95% for switched-capacitor technique.

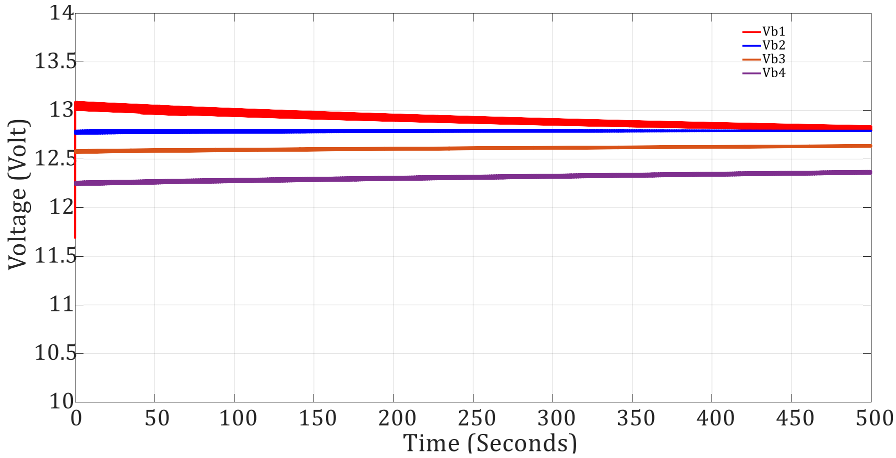

Figure 18. Four series connected batteries for switched-capacitor technique.

It is wealth to note that for either technique, voltages of lead-acid batteries can be balanced in a shorter time when the PWM pulses are increased. However, this is left for future work to be studied and implemented.

7. CONCLUSIONS

In this study, a dynamic capacitor is proposed for controlling the unbalanced voltages of lead-acid batteries that are mostly used in residence as well as small business solar power systems to back up the surplus power and to be used later mainly during the night. The details of the mathematical model of the lead-acid batteries and the operation of the dynamic capacitor technique were presented. The dynamic capacitor technique consisted of two switches in which one is on while the other is off and vice versa during each cycle of operation. The PWM is used for controlling the *ON/OFF* of both switches. The simulation was carried out using MATLAB/Simulink to validate the proposed technique. Simulation results showed the effectiveness of the proposed technique in which the voltages of all lead-acid series-connected batteries were balanced in a shorter time as other techniques can provide such as the switched-capacitor technique. The balancing voltages in two batteries reached the settling time within 100 seconds for as low as 4% differences, while these took above 500 seconds and just a 20% difference in the switched-capacitor method.

NOMENCLATURE

Symbol	Description	Symbol	Description
A_o	Constant parameters	Q_c	Ripple factor of the inductor current
A_{21}	Battery internal parameters	Q_e	Battery consumed charge in Ah
A_{22}	Battery internal parameters	R_o	Output resistance, Ω
A_p	Battery cell constants	R_{oo}	Constant parameters
C	Capacitor, F	R_1	Inductor internal resistance, Ω
C_1	Actual battery capacity, Ah	R_2	Summation of inductor and capacitor internal resistance, Ω
C_{10}	Rated charge capacity of the battery, Ah	R_{10}	Battery internal parameters
C_{in}	Filter capacitor, F	R_{20}	Battery internal parameters
D	Duty cycle	R_{i1}	First main branch resistor, Ω
DOC	Depth of charge	R_{i2}	Second main branch resistor, Ω
E_m	Battery voltage, V	S_1	First switch
E_{ma}	Battery internal voltage, V	S_2	Second switch
E_p	Parasitic branch voltage	SOC	The state-of-charge
E_{po}	*Battery cell constants*	t_{on}	Switching ON time, s
f	Switching frequency, Hertz	t_{off}	Switching OFF time, s
G_{po},	Battery cell constants	Th_e	Electrolyte temperature, Kelvin
i_c	Capacitor current, A	Th_f	Electrolyte freezing temperature
i_L	Inductor current, A	v_b	Battery voltage, V
i_{Lf}	Forced current, A	v_c	Capacitor voltage, V
i_{Lu}	Unforced inductor current, A	v_{cf}	Forced capacitor voltage, V
Im	Actual main branch current, A	v_{cu}	Unforced capacitor voltage, V
I_o	Rated battery cell current, A	v_{in}	Input voltage, V
I_p	Parasitic branch current	v_L	Inductor voltage, V
K_e	Voltage temperature coefficient of the battery, Kelvin	x_c	Capacitive reactance, Ω
L	Inductor, H	λ	Eign value
L_{in}	Filter inductor, H	ζ	Damping ratio
PWM	Pulse width modulation	τ_c	Time constant of the cell, s

REFERENCES

Alvarez-Diazcomas, A., Estévez-Bén, A.A., Rodríguez-Reséndiz, J., Martínez-Prado, M., Carrillo-Serrano, R.V., and Thenozhi, S., 2020. A Review of battery equalizer circuits for electric vehicle applications. *Energies,* 13(21: 5688), pp. 1 -29. Doi:10.3390/en13215688

Apribowo, C., Sarjiya, S., Hadi, S.P., and Wijaya , F.D., 2022. Optimal planning of battery energy storage systems by considering battery degradation due to ambient temperature: a review, challenges, and new perspective. *Batteries,* 8(12: 290), pp. 1-29, Doi:10.3390/batteries8120290

Aula, F.T., 2022. Design a reactive power compensator in smart home under variation of supply voltage of low-level distributed power system, *ZANCO. Journal of Pure and Applied Sciences,* 34(4), pp. 74-82. Doi:10.21271/ZJPAS.34.4.8

Bagalini, V., Zhao, B.Y., Wang, R.Z. and Desideri, U., 2019. Solar PV-battery-electric grid-based energy system for residential applications: system configuration and viability. *Research*, *2019*. Doi:10.34133/2019/3838603

Belmokhtar, K., Ibrahim, H., Féger, Z., Ghandour, M., 2016. Charge equalization systems for serial valve regulated lead-acid (VRLA) connected batteries in hybrid power systems applications. *Energy Procedia,* 99, pp. 277-284*.* Doi:10.1016/j.egypro.2016.10.117

Chen, T., Jin, Y., Lv, H., Yang, A., Liu, M., Chen, B., Xie, Y. and Chen, Q., 2020. Applications of lithium-ion batteries in grid-scale energy storage systems. *Transactions of Tianjin University*, *26*(3), pp.208-217. Doi:10.1007/s12209-020-00236-w

Collath, N., Tepe, B., Englberger, S., Jossen, A. and Hesse, H., 2022. Aging aware operation of lithium-ion battery energy storage systems: A review. *Journal of Energy Storage*, *55*, p.105634. Doi:10.1016/j.est.2022.105634.

Dufo-López, R., Cortés-Arcos, T., Artal-Sevil, J.S. and Bernal-Agustín, J.L., 2021. Comparison of lead-acid and li-ion batteries lifetime prediction models in stand-alone photovoltaic systems. *Applied Sciences*, *11*(3), p.1099. Doi:10.3390/app11031099.

Fortenbacher, P., Mathieu, J.L. and Andersson, G., 2017. Modeling and optimal operation of distributed battery storage in low voltage grids. *IEEE Transactions on Power Systems*, *32*(6), pp.4340-4350. Doi:10.1109/TPWRS.2017.2682339.

Hamed, H.H., Zainulabdeen, I.H., Raheem, S.S. and Mohammed, A.E., 2018. A comparison study of performance efficiency of lead-acid batteries Available in the Iraqi Markets. *International Journal of Engineering & Technology*, *7*(4.37), pp.150-152. Doi:10.14419/ijet.v7i4.37.24091

Ho, K.C., Liu, Y.H., Ye, S.P., Chen, G.J. and Cheng, Y.S., 2021. Mathematical modeling and performance evaluation of switched-capacitor-based battery equalization systems. *Electronics*, *10*(21), p.2629. Doi:10.3390/electronics10212629

IEA, 2022. Solar PV Global Supply Chains, *IEA*, Paris, https://www.iea.org/reports/solar-pv-global-supply-chains

Kavaliauskas, Ž., Šajev, I., Blažiūnas, G. and Gecevičius, G., 2023. Electronic life cycle monitoring system for various types of lead acid batteries. *Applied Sciences*, *13*(8), p.4746. Doi:10.3390/app13084746

Kim, M.Y., Kim, C.H., Kim, J.H. and Moon, G.W., 2013. A chain structure of switched capacitor for improved cell balancing speed of lithium-ion batteries. *IEEE Transactions on Industrial Electronics*, *61*(8), pp.3989-3999*.* Doi:10.1109/TIE.2013.2288195

Lipu, M.S.H., Mamun, A.A., Ansari, S., Miah, M.S., Hasan, K., Meraj, S.T., Abdolrasol, M.G., Rahman, T., Maruf, M.H., Sarker, M.R. and Aljanad, A., 2022. Battery management, key technologies, methods, issues, and future trends of electric vehicles: A pathway toward achieving sustainable development goals. *Batteries*, *8*(9), p.119. Doi:10.3390/batteries8090119

Manimekalai, P., Harikumar, R. and Raghavan, S., 2013. An overview of batteries for photovoltaic (PV) systems. *International Journal of Computer Applications*, *82*(12). Doi:10.5120/14170-2299

Maraud, H.S., Abdulbaqi, I.M. and Majeed, A.I., 2016. Design, simulation and analysis of an intelligent lead-acid battery charger fed by solar system. *Journal of Engineering and Sustainable Development*, *20*(5), pp.197-212.

May, G.J., Davidson, A. and Monahov, B., 2018. Lead batteries for utility energy storage: A review. *Journal of energy storage*, *15*, pp.145-157. Doi:10.1016/j.est.2017.11.008.

Moghaddam, A.F. and Van den Bossche, A., 2019, May. A battery equalization technique based on Ćuk converter balancing for lithium ion batteries. In *2019 8th International Conference on Modern Circuits and Systems Technologies (MOCAST)* (pp. 1-4). IEEE. Doi:10.1109/MOCAST.2019.8741779.

Pan, X., Khezri, R., Mahmoudi, A. and Muyeen, S.M., 2022. Optimal planning of solar PV and battery storage with energy management systems for Time-of-Use and flat electricity tariffs. *IET Renewable Power Generation*, *16*(6), pp.1206-1219. Doi:10.1049/rpg2.12433

Rajanna, B.V. and Kumar, M.K., 2021. Comparison study of lead-acid and lithium-ion batteries for solar photovoltaic applications. *Int. J. Power Electron. Drive Syst*, *12*(2), p.1069. Doi:10.11591/ijpeds.v12.i2.pp1069-1082

Raji, S. and Kubba, Z.M., 2020. Design and simulation of lead-acid battery. *Al-Nahrain Journal of Science*, *23*(3), pp.39-44.

Rasheed, L., 2020. Bat algorithm based an adaptive PID controller design for buck converter model, *Journal of Engineering,* 26(7), pp. 62–82. Doi:10.31026/j.eng.2020.07.05

Salameh, T., Kumar, P.P., Olabi, A.G., Obaideen, K., Sayed, E.T., Maghrabie, H.M. and Abdelkareem, M.A., 2022. Best battery storage technologies of solar photovoltaic systems for desalination plant using the results of multi optimization algorithms and sustainable development goals. *Journal of Energy Storage*, *55*, p.105312.Doi:10.1016/j.est.2022.105312

Samanta, A., and Chowdhuri, S., 2021. Active cell balancing of lithium-ion battery pack using dual DC-DC converter and auxiliary lead-acid battery. *Journal of Energy Storage*, *33*, P. 102109. Doi:10.1016/j.est.2020.102109

Shang, Y., Xia, B., Lu, F., Zhang, C., Cui, N. and Mi, C.C., 2016. A switched-coupling-capacitor equalizer for series-connected battery strings. *IEEE Transactions on Power Electronics*, *32*(10), pp.7694-7706. *Doi:1*0.1109/TPEL.2016.2638318

Victoria, M., Haegel, N., Peters, I.M., Sinton, R., Jäger-Waldau, A., del Canizo, C., Breyer, C., Stocks, M., Blakers, A., Kaizuka, I. and Komoto, K., 2021. Solar photovoltaics is ready to power a sustainable future. *Joule*, *5*(5), pp.1041-1056.Doi:10.1016/j.joule.2021.03.005

Wang, S., Kang, L., Guo, X., Wang, Z. and Liu, M., 2017. A novel layered bidirectional equalizer based on a buck-boost converter for series-connected battery strings. *Energies*, *10*(7), p.1011. Doi:10.3390/en10071011

Wang, X., Tan, Z., Cai, L., Lei, G. and Dai, N., 2023. Bi-Directional cuk equalizer-based li-ion battery pack equalization control strategy research. *World Electric Vehicle Journal*, *14*(4), p.86. Doi:10.3390/wevj14040086

Wu, X., Tang, Z., Stroe, D.I. and Kerekes, T., 2022. Overview and Comparative Study of Energy Management Strategies for Residential PV Systems with Battery Storage. *Batteries*, *8*(12), p.279. Doi:10.3390/batteries8120279

Ye, Y., Cheng, K.W.E., Fong, Y.C., Xue, X. and Lin, J., 2016. Topology, modeling, and design of switched-capacitor-based cell balancing systems and their balancing exploration. *IEEE Transactions on Power Electronics*, *32*(6), pp.4444-4454.Doi:10.1109/TPEL.2016.2584925

Zau, A.T.P., Lencwe, M.J., Chowdhury, S.D. and Olwal, T.O., 2022. A battery management strategy in a lead-acid and lithium-ion hybrid battery energy storage system for conventional transport vehicles. *Energies*, *15*(7), p.2577. Doi:10.3390/en15072577

Zhang, Y., Kim, M., Wang, L., Verlinden, P. and Hallam, B., 2021. Design considerations for multi-terawatt scale manufacturing of existing and future photovoltaic technologies: challenges and opportunities related to silver, indium and bismuth consumption. *Energy & Environmental Science*, *14*(11), pp.5587-5610. Doi:10.1039/D1EE01814K

Zheng, J., Chen, J. and Ouyang, Q., 2018. Variable universe fuzzy control for battery equalization. *Journal of Systems Science and Complexity*, *31*, pp.325-342. Doi.10.1007/s11424-018-7366-7.